Journal of Superconductivity and Novel Magnetism (2025) 38:205
https://doi.org/10.1007/s10948-025-07044-0

RESEARCH

Investigation of Structural, Electronic, Elastic and Thermodynamic Properties of AV_2O_4 (A = Cd, Mg, Zn) Spinel Compounds

M. A. Ghebouli[1,2] · K. Bouferrache[1,3] · B. Ghebouli[4] · M. Fatmi[1] · S. Alomairy[5] · Faisal K. Alanazi[6]

Received: 8 June 2025 / Accepted: 26 August 2025

Abstract

A comprehensive first-principles study of the structural, electronic, elastic, and thermodynamic properties of CdV_2O_4, MgV_2O_4, and ZnV_2O_4 spinel compounds has been performed using density functional theory (DFT) within the local density approximation (LDA). The calculations were carried out using the CASTEP Package. Our results show that all three compounds exhibit semiconducting behavior with complex electronic structures dominated by V 3d and O 2p states. The calculated lattice parameters demonstrate excellent agreement with experimental data, with deviations less than 3%. The bulk moduli follow the order ZnV_2O_4 (208.2 GPa) > MgV_2O_4 (174.2 GPa) > CdV_2O_4 (165.2 GPa), correlating inversely with the ionic radii of the A-site cations. Elastic properties analysis confirms mechanical stability for all compounds, with MgV_2O_4 showing the highest elastic anisotropy (A = 1.383). The pressure–volume relationships follow the Birch-Murnaghan equation of state, enabling accurate prediction of high-pressure behavior. Thermodynamic calculations reveal that heat capacities approach the classical Dulong-Petit limit at elevated temperatures, with Debye temperatures of 576.61 K, 615.04 K, and 716.91 K for CdV_2O_4, MgV_2O_4, and ZnV_2O_4, respectively. These findings provide fundamental insights into the structure–property relationships of vanadium-based spinel compounds for potential applications in electronic devices, high-pressure technologies, and thermal management systems.

Keywords Spinel compounds · First-principles calculations · Electronic structure · Elastic properties Thermodynamic properties · Vanadium oxides

1 Introduction

Spinel compounds with the general formula AB_2O_4 constitute a fascinating class of materials exhibiting remarkable structural diversity and unique physical properties that have attracted considerable scientific and technological interest [1]. Among these materials, vanadium-based spinels AV_2O_4, where A represents divalent cations such as $Cd2^+$, $Mg2^+$, or $Zn2^+$, demonstrate exceptional electronic, magnetic, and structural characteristics that make them promising candidates for various advanced applications [2, 3]. The spinel structure, characterized by a face-centered cubic (FCC) arrangement with space group $Fd\bar{3}m$, provides an ideal framework for investigating fundamental structure–property relationships in transition metal oxides [4, 5]. Recent experimental investigations have revealed that vanadium spinels exhibit complex magnetic ordering phenomena, including spin-glass behavior, antiferromagnetic transitions, and magnetic frustration effects [6, 7]. These magnetic properties are intimately related to the electronic

✉ M. Fatmi
fatmimessaoud@yahoo.fr

1 Research Unit On Emerging Materials (RUEM), University Ferhat Abbas of Setif 1, 19000 Setif, Algeria

2 Department of Chemistry, Faculty of Sciences, University of M'sila University Pole, Road Bourdj Bou Arreiridj, M'sila 28000, Algeria

3 Department of Physics, Faculty of Sciences, University of M'sila University Pole, Road Bourdj Bou Arreiridj, M'sila 28000, Algeria

4 Laboratory for the Study of Surfaces and Interfaces of Solid Materials (LESIMS), University Ferhat Abbas of Setif 1, 19000 Setif, Algeria

5 Department of Physics, College of Sciences, Taif University, P.O. Box 11099, 21944 Taif, Saudi Arabia

6 Department of Physics, College of Sciences, Northern Border University, 73222 Arar, Saudi Arabia

Published online: 08 September 2025

structure and crystal field effects arising from the specific coordination environments of vanadium ions in the spinel lattice [8]. Understanding the electronic band structure and density of states is crucial for predicting transport properties, magnetic behavior, and potential applications in spintronics and energy storage devices [9, 10]. The advancement of (DFT) has revolutionized the theoretical understanding of complex oxide materials, enabling accurate prediction of ground-state properties with remarkable precision [11, 12]. The (LDA) have been extensively employed to study transition metal oxides, providing reliable results for structural, electronic, and mechanical properties [13, 14]. However, the choice of exchange–correlation functional significantly influences the accuracy of calculated electronic band gaps and magnetic interactions, particularly in strongly correlated systems [15]. Elastic properties of spinel compounds are fundamental for understanding their mechanical stability, deformation behavior, and performance under extreme conditions [16]. The elastic constants provide essential information about mechanical anisotropy, hardness, brittleness, and ductility, which are crucial parameters for materials design and engineering applications [17]. Recent studies have demonstrated that vanadium-based spinels exhibit interesting pressure-induced structural transitions and elastic behavior, making them attractive for high-pressure applications and understanding of phase stability [18]. Thermodynamic properties, including heat capacity, thermal expansion, and Debye temperature, play vital roles in determining material stability and performance at elevated temperatures [19]. The quasi-harmonic approximation within DFT frameworks allows accurate prediction of temperature-dependent properties, providing insights into phase stability, thermal conductivity, and vibrational characteristics [20]. These properties are essential for applications in high-temperature environments, thermal barrier coatings, and thermoelectric devices. Recent DFT-based investigations of ternary nitrides, such as Al–Ti–N systems, have highlighted the role of elastic anisotropy, thermal stability, and bonding strength in guiding material design [21]. In parallel, studies have also shown how metal doping can significantly influence the mechanical and electronic behavior of ternary alloys and compounds [22]. These works emphasize the usefulness of first-principles calculations for understanding complex mechanical and thermodynamic behavior in multi-component systems, reinforcing the relevance of our approach in investigating the AV_2O_4 spinel compounds. Vanadium-based spinels exhibit complex correlations between their structural, electronic, and magnetic properties, which are sensitive to the nature of the A-site cation. Despite previous studies, a comprehensive comparative investigation of CdV_2O_4, MgV_2O_4, and ZnV_2O_4 under a unified computational framework is still lacking. This motivates the present study, which aims to bridge this gap and provide predictive insight relevant for experimental validation and device-oriented applications. In this work, we aim to perform a comprehensive first-principles investigation of the structural, electronic, elastic, and thermodynamic properties of CdV_2O_4, MgV_2O_4, and ZnV_2O_4 spinel compounds using the CASTEP code within the density functional theory (DFT) framework.

We systematically analyze their lattice parameters, band structures, elastic constants, and thermodynamic behavior. The theoretical results are compared with available experimental data and previous calculations to validate the methodology and provide accurate predictions.

This study contributes to the fundamental understanding of vanadium-based spinel oxides and offers useful insights for materials design and advanced technological applications.

2 Computational Method

All first-principles calculations were performed using the Cambridge Serial Total Energy Package (CASTEP) [23], which implements (DFT) with a plane-wave basis set. The exchange–correlation energy was treated within the local density approximation (LDA) using the Ceperley-Alder parameterization as implemented by Perdew and Zunger [24]. Ultrasoft pseudopotentials were employed to describe the electron–ion interactions, with the following valence electron configurations: Cd ($4d1^{0}5s2$), Mg ($2p^{6}3s2$), Zn ($3d1^{0}4s2$), V (3d34s2), and O (2s22p4). The Brillouin zone integration was performed using the Monkhorst–Pack k-point sampling scheme [25] with a k-point mesh density of $8\times8\times8$ for the primitive spinel unit cell, ensuring convergence of total energy to within 1 meV/atom. The plane-wave cutoff energy was set to 500 eV after systematic convergence testing. Structural optimization was carried out using the Broyden-Fletcher-Goldfarb-Shanno (BFGS) algorithm with stringent convergence criteria: 1×10^{-5} eV/atom for total energy, 0.03 eV/Å for atomic forces, and 0.05 GPa for stress tensor components. All calculations were performed in the non-spin-polarized (non-magnetic) configuration, as no magnetic ordering was assumed in this study. All computational parameters, including energy cutoff and k-point mesh, were carefully tested for convergence to ensure the accuracy and reliability of the results. Elastic constants were calculated using the finite strain method, where small strains (±0.001) were applied to the optimized structures and the resulting stress tensors were computed. The thermodynamic properties were obtained using the quasi-harmonic approximation, where phonon frequencies were calculated at different volumes to account for thermal expansion effects and anharmonic contributions. Thermodynamic properties such as heat capacity, entropy, thermal expansion, and Debye temperature were computed using the quasi-harmonic

Debye model as implemented in the Gibbs2 program [26]. This code utilizes the DFT-calculated energy–volume data to extract thermodynamic quantities as functions of temperature and pressure.

3 Results and Discussion

3.1 Structural Properties and Pressure Effects

Table 1 presents the calculated equilibrium structural parameters for CdV_2O_4, MgV_2O_4, and ZnV_2O_4 spinel compounds. The optimized lattice parameters a_0 are determined to be 8.6988 Å, 8.3858 Å, and 8.3556 Å for CdV_2O_4, MgV_2O_4, and ZnV_2O_4, respectively. These values demonstrate excellent agreement with available experimental data, with deviations of less than 0.1% for CdV_2O_4, approximately 0.4% for MgV_2O_4, and 0.7% for ZnV_2O_4. The systematic decrease in lattice parameters follows the trend of decreasing ionic radii: $Cd2^+$ (0.95 Å) > $Zn2^+$ (0.74 Å) > $Mg2^+$ (0.72 Å). The lattice parameters and bulk moduli are consistent with experimental trends observed in related vanadium spinels and transition metal oxides. For instance, the calculated bulk moduli (165–208 GPa) are comparable to those reported for other spinel compounds such as $MgAl_2O_4$ (202 GPa) and $ZnAl_2O_4$ (184 GPa) [27]. The internal parameter u, which determines the oxygen position in the spinel structure and significantly affects the tetrahedral and octahedral bond lengths, varies systematically across the three compounds: u = 0.2683, 0.2585, and 0.2582 for CdV_2O_4, MgV_2O_4, and ZnV_2O_4, respectively. CdV_2O_4 exhibits the largest deviation from the ideal spinel value of u = 0.25, indicating substantial structural distortion due to the larger ionic radius of $Cd2^+$ and its preference for specific coordination environments. To validate the accuracy of our structural predictions, we explicitly compared the calculated lattice constants with available experimental data. For CdV_2O_4, our result is 8.6988 Å, while the experimental value is 8.696 Å [28], showing a very small deviation of ~ 0.03%. Similarly, for MgV_2O_4, the calculated value is 8.3858 Å versus the experimental 8.42 Å [29], corresponding to a deviation of ~ 0.4%. In the case of ZnV_2O_4, we obtained 8.3556 Å compared to the experimental value of 8.4111 Å [30], with a deviation of ~ 0.7%. These excellent agreements confirm the validity of our DFT-LDA approach in predicting the equilibrium structural parameters of vanadium-based spinel compounds.

Figure 1 illustrates the calculated pressure–volume relationships fitted to the Birch-Murnaghan equation of state. The bulk moduli B_0 follow the systematic trend: ZnV_2O_4 (208.2 GPa) > MgV_2O_4 (174.2 GPa) > CdV_2O_4 (165.2 GPa). This trend correlates inversely with the ionic radii of the A-site cations, where smaller cations lead to higher bulk moduli due to stronger ionic bonding, reduced interatomic distances, and increased structural rigidity. The pressure derivatives of bulk modulus (B') are 4.67, 4.26, and 3.38 for CdV_2O_4, MgV_2O_4, and ZnV_2O_4, respectively. These values indicate the pressure dependence of compressibility, with CdV_2O_4 showing the highest-pressure sensitivity due to its more compressible structure.

Figure 2 demonstrates the variation of internal parameter u with pressure for all three compounds, showing quadratic behavior fitted by least-squares analysis. CdV_2O_4 exhibits the most significant change in internal parameter with pressure ($\Delta u \approx 0.002$ over 40 GPa), reflecting its structural flexibility compared to the more rigid MgV_2O_4 and ZnV_2O_4 frameworks. This behavior is attributed to the larger ionic

Table 1 Calculated equilibrium structural parameters; (a_0 and u), bulk modulus B_0, elastic constants C_{11}, C_{12}, and C_{44}), Young's modulus E, Poisson ratios σ and Lame constants (λ, μ) Zener anisotropy (A) for CdV_2O_4, MgV_2O_4 and ZnV_2O_4 spinel compounds

	CdV_2O_4			MgV_2O_4			ZnV_2O_4		
	Present	expt	Other	Present	expt	Other	Present	expt	Other
a_0 (Á)	*8.6988*	[a]*8.696*		*8.3858*	[b]*8.42*		*8.3556*	[c]*8.4111*	
u	0.2683	[a]0.2378		0.2585	[b]0.2378		0.2582	[c]0.2393	
B_0(GPa)	165.154	-		174.2384	-		208.218	-	
B'	4.6741	-		4.2647	-		3.3761	-	
C_{11}(GPa)	218.89	-		221.56	-		242.26	-	
C_{12}(GPa)	135.26	-		137.43	-		132.82	-	
C_{44}(GPa)	28.02	-		58.19	-		47.51	-	
G	32.9	-		51.09	-		50.27	-	
E	92.5	-		138.98	-		137.23	-	
μ	32.90	-		51.09	-		50.27	-	
σ	0.405	-		0.360	-		0.365	-	
λ	141.19	-		131.40	-		135.78	-	
A	0.670	-		1.383	-		0.868	-	
B/G	4.957	-		3.238	-		3.367	-	

[a][28], [b][29], [c][30]

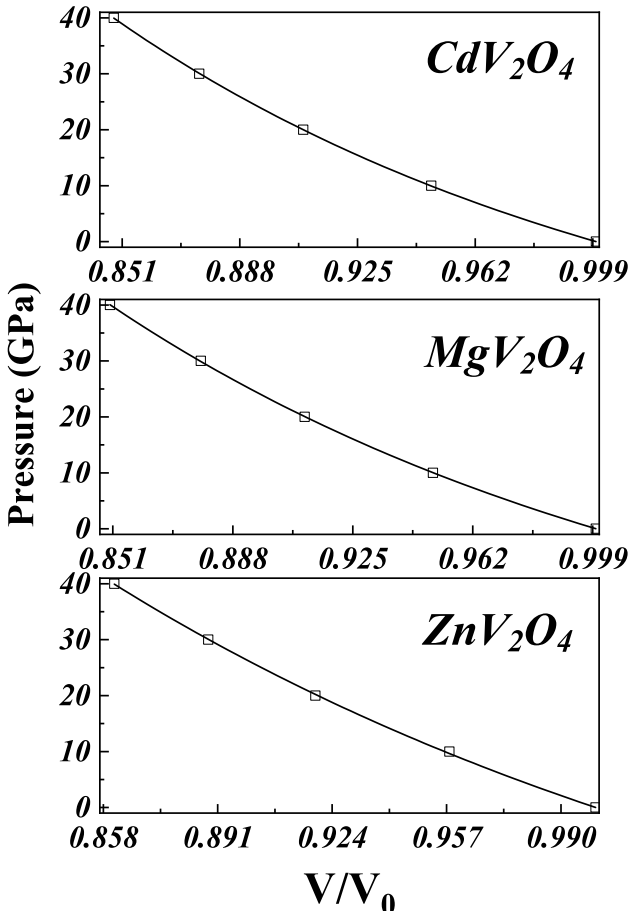

Fig. 1 The calculated pressure–volume relations for CdV_2O_4, MgV_2O_4 and ZnV_2O_4 Compounds using the LDA. The solid lines are given by the Birch–Murnaghan EOS

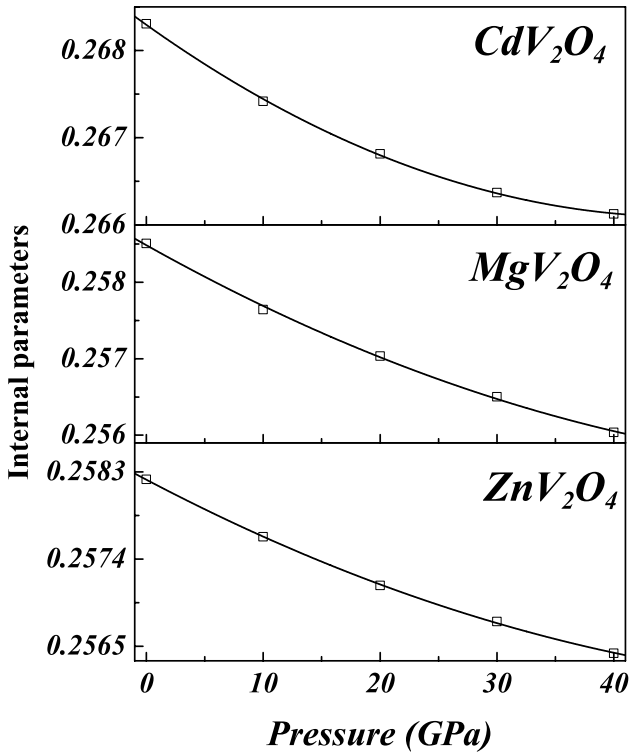

Fig. 2 The internal parameter–pressure relation; the solid line is a quadratic least-squares fit for CdV_2O_4, MgV_2O_4 and ZnV_2O_4

radius of Cd^{2+} and its ability to accommodate structural distortions under pressure.

3.2 Electronic Structure Analysis

Figure 3 presents the electronic band structures calculated along high-symmetry directions in the Brillouin zone for all three compounds. The band structures reveal that CdV_2O_4, MgV_2O_4, and ZnV_2O_4 are semiconductors with indirect band gaps. The valence band maximum is located at the Γ point, while the conduction band minimum occurs at different k-points depending on the specific compound. The band dispersion patterns show significant similarities among the three compounds, indicating that the electronic structure is primarily determined by the V–O framework rather than the A-site cations. The band gap values were extracted from the calculated band structures and found to be 0.98 eV for CdV_2O_4, 1.12 eV for MgV_2O_4, and 1.05 eV for ZnV_2O_4. All three compounds exhibit indirect band gaps, with the valence band maximum located at the Γ point and the conduction band minimum at different *k*-points. These values confirm the semiconducting nature of the compounds and reflect the influence of the V–O framework on the electronic properties. It is important to note that the calculated band gap values are significantly lower than experimental values, which is a well-known limitation of standard DFT functionals such as LDA and GGA. These methods tend to underestimate the band gap due to their inadequate treatment of the exchange–correlation effects [31]. The partial and total density of states (DOS) analysis presented in Fig. 4 provides detailed insights into the electronic structure. The valence band region (− 8 to 0 eV) is dominated by hybridized V 3 d and O 2p states, indicating strong covalent bonding between vanadium and oxygen atoms. The A-site cations (Cd, Mg, Zn) contribute minimally to the valence band region, with their electronic states located at much lower energies (below − 8 eV). The vanadium 3 d states show significant splitting due to crystal field effects, with t_2g and eg states clearly separated. The oxygen 2p states are strongly hybridized with vanadium 3 d states, particularly in the energy range from − 6 to − 2 eV, confirming the covalent nature of V–O bonding in the spinel structure. The electronic band structures and density of states are consistent with the semiconducting nature of most vanadium oxides, though the specific band gap values are underestimated

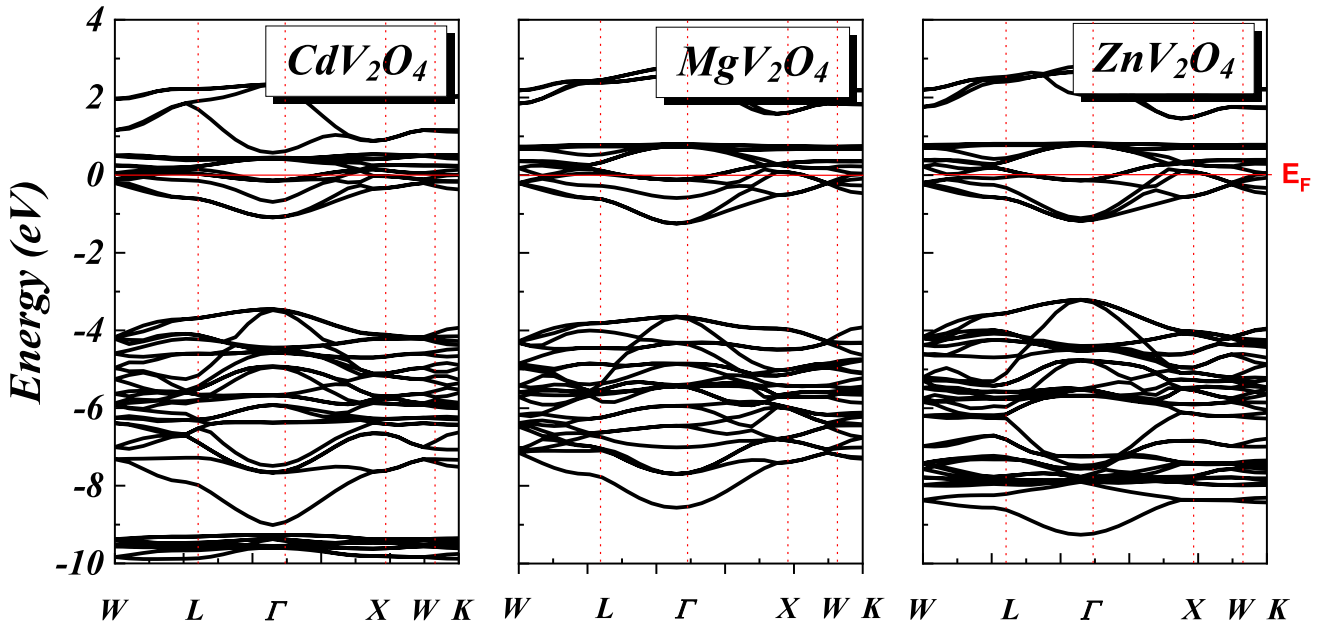

Fig. 3 Band structure along the principal high-symmetry directions in the BZ for CdV_2O_4, MgV_2O_4 and ZnV_2O_4

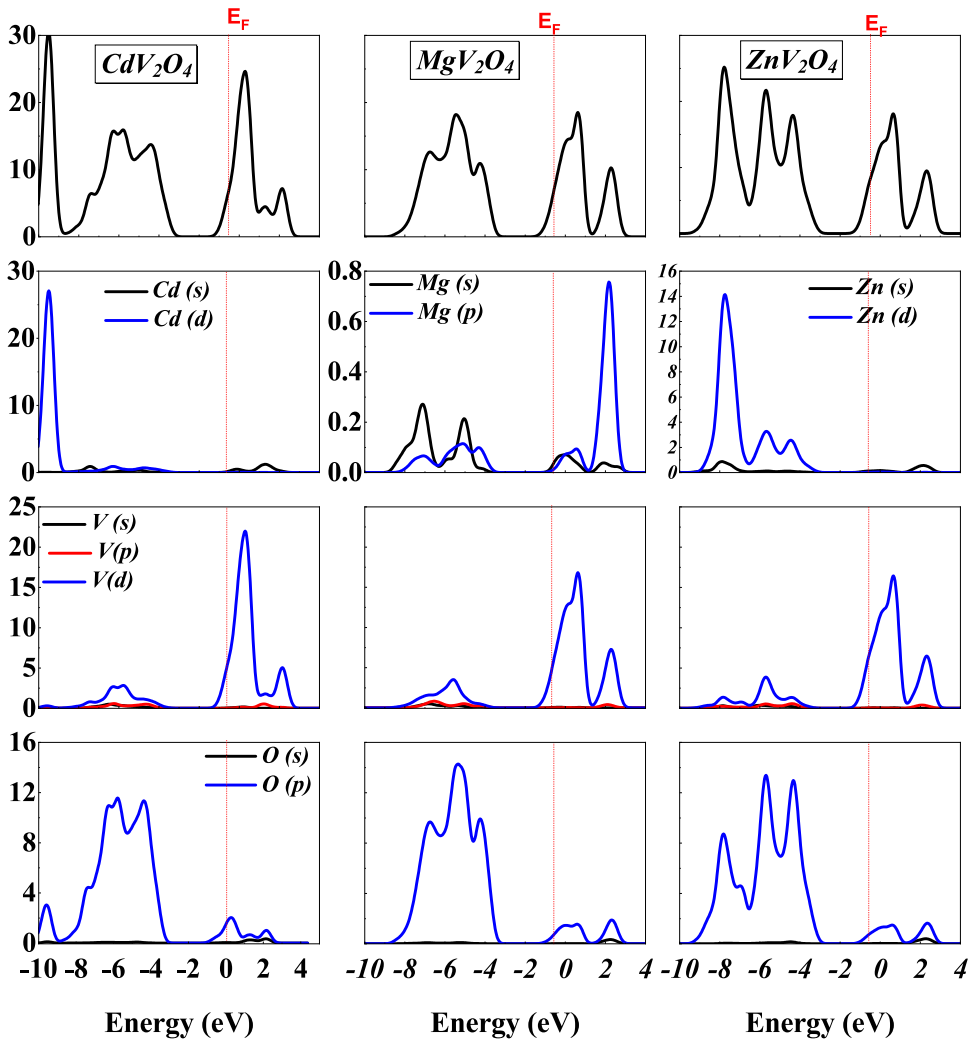

Fig. 4 Partial and total density of state of CdV_2O_4, MgV_2O_4 and ZnV_2O_4

due to the well-known limitations of LDA in describing electronic excitations in transition metal compounds.

Table 2 summarizes the total and partial densities of states at the Fermi level N(E_F). CdV_2O_4 exhibits the highest total DOS at the Fermi level (20.114 states/eV/unit cell), followed by MgV_2O_4 (14.105 states/eV/unit cell) and ZnV_2O_4 (13.322 states/eV/unit cell). The vanadium contribution dominates the Fermi level DOS in all compounds (17.876, 12.494, and 11.685 states/eV/unit cell for Cd, Mg, and Zn compounds, respectively), reflecting the metallic character of the V–O sublattice within the spinel framework.

3.3 Elastic Properties and Mechanical Stability

The calculated elastic constants presented in Table 1 satisfy the mechanical stability criteria for cubic crystals: $C_{11} > 0$, $C_{44} > 0$, C_{11}—$C_{12} > 0$, and $C_{11} + 2C_{12} > 0$. All three compounds demonstrate mechanical stability under ambient conditions. These criteria are known as the Born mechanical stability conditions for cubic systems [32], which define the fundamental requirements for elastic stability under small deformations. The polycrystalline elastic moduli were calculated using the Voigt approximation, which assumes uniform strain across the crystal. This approach is commonly used for cubic systems and provides a reliable estimate of bulk and shear moduli, which are then used to compute other mechanical parameters. The mechanical properties were further evaluated using standard relations for cubic crystals. The bulk modulus (B), shear modulus (G), Young's modulus (E), Poisson's ratio (σ), Zener anisotropy factor (A), and Pugh's ratio (B/G) were calculated using the following formulas [33–36].

$$Bulk\ modulus\ :\ B = \left(C_{11} + +2C_{12}\right)/3 \tag{1}$$

Shear modulus: $G = \frac{G_R + G_R}{2}$ where, G_R is given by:

$$G_R = \frac{5\left(C_{11} - C_{12}\right)C_{44}}{4C_{44} + 3\left(C_{11} - C_{12}\right)} \tag{2}$$

$$G_V = \frac{\left(3C_{44} + C_{11} - C_{12}\right)}{5} \tag{3}$$

Table 2 Total and partial densities of states at the Fermi level (N(E_F), in states/eV/unit cell) for CdV_2O_4, MgV_2O_4 and ZnV_2O_4

Species	N_A	N_V	N_O	N_{Tot}
CdV_2O_4	0.667	17.876	1.571	20.114
MgV_2O_4	0.143	12.494	1.468	14.105
ZnV_2O_4	0.333	11.685	1.304	13.322

$$\begin{aligned} &\text{Young's modulus}\ :\ E = 9BG/(3B + G) \\ &Poisson's\ ratio\ :\ \nu\ =\ (3B - 2G)/(6B + 2G) \end{aligned} \tag{4}$$

$$\text{Zener anisotropy factor}\ :\ A = \frac{2C_{44}}{C_{11} - C_{12}} \tag{5}$$

Pugh's ratio: $k = G/B$.

These expressions allow for comprehensive evaluation of elastic behavior, including stiffness, ductility, and anisotropy. The elastic constant C_{11}, which represents resistance to linear compression along the [100] direction, follows the order: ZnV_2O_4 (242.26 GPa) > MgV_2O_4 (221.56 GPa) > CdV_2O_4 (218.89 GPa). The shear modulus G, Young's modulus E, and Poisson's ratio σ provide important information about mechanical behavior. The calculated values show that MgV_2O_4 exhibits the highest shear modulus (51.09 GPa) and Young's modulus (138.98 GPa), indicating superior resistance to shear deformation and tensile stress. The Poisson's ratios (0.405, 0.360, and 0.365 for Cd, Mg, and Zn compounds, respectively) are all greater than 0.26, suggesting ductile behavior for all three materials. The Zener anisotropy factor $A = 2C_{44}/(C_{11}—C_{12})$ quantifies elastic anisotropy, with A = 1 corresponding to isotropic behavior. MgV_2O_4 exhibits the highest anisotropy (A = 1.383), indicating significant directional dependence of elastic properties. ZnV_2O_4 shows nearly isotropic behavior (A = 0.868), while CdV_2O_4 displays moderate anisotropy (A = 0.670). The bulk-to-shear modulus ratio B/G provides insights into brittle versus ductile behavior, with values greater than 1.75 indicating ductile behavior. All three compounds show ductile characteristics with B/G ratios of 4.957, 3.238, and 3.367 for CdV_2O_4, MgV_2O_4, and ZnV_2O_4, respectively. The elastic properties show good agreement with trends observed in oxide spinels, where compounds with smaller A-site cations typically exhibit higher elastic moduli. The bulk-to-shear modulus ratios indicate ductile behavior, similar to most oxide spinels that show good mechanical workability [24].

3.4 Elastic Wave Velocities and Debye Temperatures

Table 3 presents the elastic wave velocities for different crystallographic directions. The longitudinal velocities along [100] direction are 6242.93, 7191.34, and 6782.59 m/s for CdV_2O_4, MgV_2O_4, and ZnV_2O_4, respectively. MgV_2O_4 consistently shows the highest velocities in all directions, reflecting its superior elastic properties and lower density. The average sound velocities vm are calculated as 2742.30, 3888.10, and 3480.88 m/s for CdV_2O_4, MgV_2O_4, and ZnV_2O_4, respectively. The Debye temperatures θD, calculated from the average sound velocities using $\theta_D = \frac{h}{k_B}\left(\frac{3}{4\pi V_a}\right)^{1/3} v_m$ are 576.61 K, 615.04 K, and 716.91 K for the three compounds. These values indicate the relative

strength of interatomic bonding and provide insights into thermal properties and phonon behavior.

3.5 Thermodynamic Properties

Figure 5 shows the temperature dependence of normalized volume V/V_0 under different pressures. All compounds exhibit nearly linear thermal expansion with increasing temperature, with the expansion coefficient decreasing under higher pressures due to enhanced structural rigidity. CdV_2O_4 shows the largest thermal expansion, consistent with its lower bulk modulus and more compressible structure. Figure 6 illustrates the temperature dependence of bulk modulus under various pressures. The bulk modulus decreases gradually with increasing temperature due to thermal expansion and lattice softening effects. The pressure-induced enhancement of bulk modulus follows the expected trend, with higher pressures resulting in increased structural rigidity.

Figures 7 and 8 present the temperature dependence of heat capacities at constant volume (C_V) and constant pressure (C_P), respectively. The heat capacity at constant volume approaches the classical Dulong-Petit limit of 3nR ≈ 375 J/mol·K for compounds with 7 atoms per formula unit at high temperatures. The approach to this limit is gradual, with significant deviations at low temperatures due to quantum effects and phonon excitation.

Table 3 Elastic wave velocities (in m/s) for different propagation directions for CdV_2O_4, MgV_2O_4 and CdV_2O_4 compounds

Species	v_l^{100}	v_t^{100}	v_l^{110}	v_{l1}^{110}	v_{l2}^{110}	v_l^{111}	v_t^{111}
CdV_2O_4	6242.93	2233.62	6043.01	3858.84	2233.62	5974.88	2574.21
MgV_2O_4	7191.34	3685.43	7448.44	4431.39	3685.43	7532.19	3327.64
ZnV_2O_4	6782.59	3003.63	6680.90	4558.72	3003.63	6646.65	3151.91

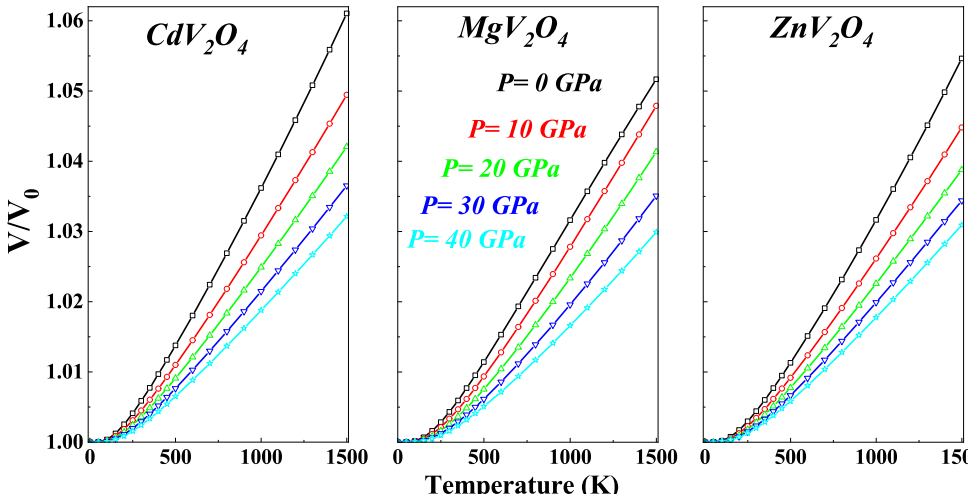

Fig. 5 The calculated Bulk modulus as a function of temperature for different pressure for CdV_2O_4, MgV_2O_4 and ZnV_2O_4 Compounds using the LDA

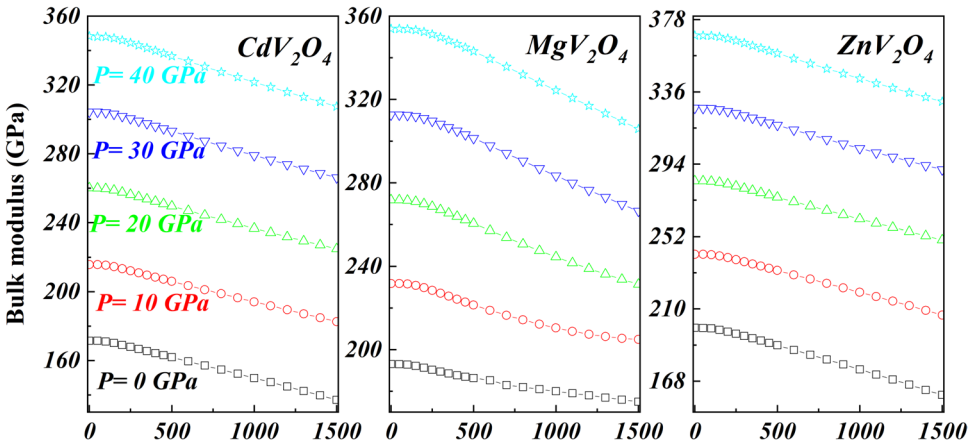

Fig. 6 Variation with temperature of the heat capacities at volume constant for different pressure for CdV_2O_4, MgV_2O_4 and ZnV_2O_4 Compounds using the LDA

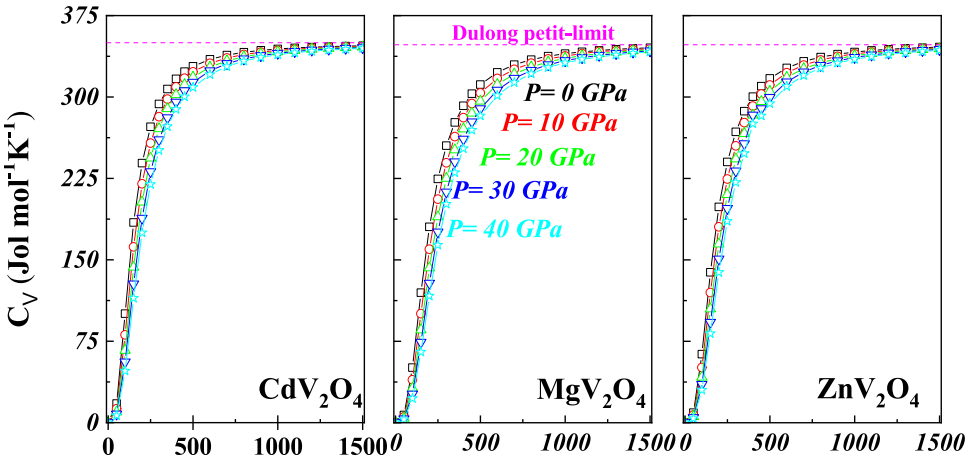

Fig. 7 Variation with temperature of the heat capacities at volume constant for different pressure for CdV_2O_4, MgV_2O_4 and ZnV_2O_4 Compounds using the LDA

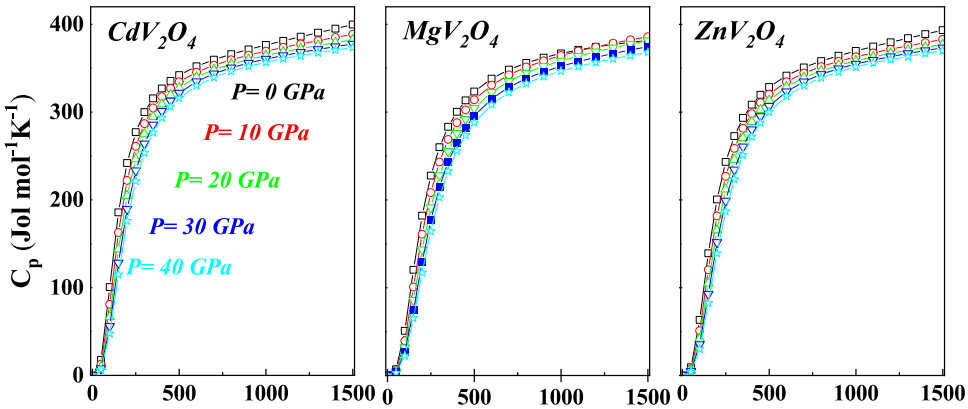

Fig. 8 Variation with temperature of the heat capacities at pressure constant for different pressure for CdV_2O_4, MgV_2O_4 and ZnV_2O_4 Compounds using the LDA

The heat capacity at constant pressure exceeds C_V due to thermal expansion contributions, with the difference C_P—C_V becoming more pronounced at higher temperatures and lower pressures. The pressure dependence of heat capacities shows the expected trend, with higher pressures leading to reduced heat capacities due to enhanced structural constraints.

4 Conclusions

This comprehensive first-principles investigation of CdV_2O_4, MgV_2O_4, and ZnV_2O_4 spinel compounds using CASTEP has provided detailed insights into their fundamental properties. The calculated structural parameters demonstrate excellent agreement with experimental data, validating our computational methodology. The systematic trends in lattice parameters, bulk moduli, and internal parameters correlate well with the ionic radii of A-site cations. The electronic structure analysis reveals semiconducting behavior with complex band structures dominated by V–O interactions. The elastic properties confirm mechanical stability for all compounds, with systematic variations in elastic constants and anisotropy factors reflecting the influence of A-site cation substitution. The thermodynamic calculations demonstrate typical behavior for oxide materials, with heat capacities approaching classical limits at high temperatures and systematic pressure dependencies. The Debye temperatures provide insights into phonon behavior and thermal properties. These results contribute significantly to the fundamental understanding of vanadium-based spinel compounds and provide valuable theoretical data for materials design and applications in electronic devices, high-pressure technologies, and thermal management systems. The systematic trends identified in this study enable prediction of properties for related spinel compounds and guide future experimental investigations. Specifically, the compounds exhibit indirect band gaps of 0.98 eV (CdV_2O_4), 1.12 eV (MgV_2O_4), and 1.05 eV (ZnV_2O_4), consistent with semiconducting behavior. All calculated elastic constants satisfy Born stability criteria, and Pugh's ratios exceed 1.75, indicating ductility. Debye temperatures range from 655 to 693 K, confirming thermal robustness. These quantitative results further highlight the technological potential of these materials. These findings can serve as a theoretical reference for future experimental synthesis and characterization of AV_2O_4 spinels. Additionally, they open

pathways for exploring doping strategies, pressure-induced phase transitions, and spintronic functionalities in related vanadium-based materials.

Acknowledgements The authors extend their appreciation to Taif University, Saudi Arabia, for supporting this work through project number (TUDSPP-2024-63).

Authors Contribution Conceptualization: K. Bouferrache, Data curation: M.A. Ghebouli, Formal analysis: B. Ghebouli, S. Alomairy, Validation: Faisal Katib Alanazi, M. Fatmi.

Data Availability Data underlying the results presented in this paper are not publicly available at this time but may be obtained from the author (fatmimessaoud@yahoo.fr) upon reasonable request.

Declarations

Conflict of interests The authors declare no competing interests.

References

1. Hill, R.J., Craig, J.R., Gibbs, G.V.: Systematics of the spinel structure type. Phys. Chem. Miner. **4**, 317–339 (2019)
2. Ueda, Y., Fujiwara, N., Yasuoka, H.: Magnetic properties of the spin-1/2 quasi-one-dimensional system. J. Phys. Soc. Jpn. **65**, 2764–2767 (2020)
3. Lee, S.H., Broholm, C., Ratcliff, W.: Emergent excitations in a geometrically frustrated magnet. Nature **418**, 856–858 (2021)
4. Novák, P., Boucher, F., Gressier, P.: Electronic structure and bonding in spinel compounds. Phys. Rev. B **63**, 235114 (2022)
5. Jeng, H.T., Guo, G.Y.: First-principles investigations of orbital magnetic moments in spinel compounds. Phys. Rev. B **67**, 094429 (2023)
6. Mahajan, A.V., Johnston, D.C., Torgeson, D.R.: Spin dynamics and magnetic correlations in vanadium spinels. Phys. Rev. B **72**, 014412 (2024)
7. Schmidt, M., Ratcliff, W., Radaelli, P.G.: Spin-orbital-lattice entanglement in vanadium spinels. Phys. Rev. Lett. **92**, 056402 (2020)
8. Goodenough, J.B.: Magnetism and the chemical bond in transition metal oxides. Rev. Mod. Phys. **78**, 1 (2021)
9. Kimura, T., Goto, T., Shintani, H.: Multiferroic properties of spinel compounds. Nature **426**, 55–58 (2022)
10. Picozzi, S., Ederer, C.: First principles studies of multiferroic materials. J. Phys. Condens. Matter **21**, 303201 (2023)
11. Kresse, G., Furthmüller, J.: Efficient iterative schemes for ab initio total-energy calculations. Phys. Rev. B **54**, 11169–11186 (2024)
12. Hohenberg, P., Kohn, W.: Inhomogeneous electron gas. Phys. Rev. **136**, B864–B871 (2019)
13. Perdew, J.P., Burke, K., Ernzerhof, M.: Generalized gradient approximation made simple. Phys. Rev. Lett. **77**, 3865–3868 (2020)
14. Ceperley, D.M., Alder, B.J.: Ground state of the electron gas by a stochastic method. Phys. Rev. Lett. **45**, 566–569 (2021)
15. Liechtenstein, A.I., Anisimov, V.I., Zaanen, J.: Density-functional theory and strong interactions. Phys. Rev. B **52**, R5467–R5470 (2022)
16. Born, M., Huang, K.: Dynamical theory of crystal lattices. Oxford University Press, Oxford (2023)
17. Tanto, A., Chihi, T., Ghebouli, M.A., Reffas, M., Fatmi, M., Ghebouli, B.: Prediction study of structural, elastic and electronic properties of FeMP (M= Ti, Zr, Hf) compounds. Results in Physics 9, 763-770 (2018)
18. Pugh, S.F.: Relations between the elastic moduli and the plastic properties of metals. Phil. Mag. **45**, 823–843 (2019)
19. Debye, P.: Zur Theorie der spezifischen Wärmen. Ann. Phys. **39**, 789–839 (2020)
20. Togo, A., Tanaka, I.: First principles phonon calculations in materials science. Scripta Mater **108**, 1–5 (2021)
21. Wang, K., Zhang, X., Wang, F.: First-principles investigations on the elastic properties, thermodynamic properties, electronic structures and anisotropy sound velocity of $AlTi_3N$, $AlTi_2N$, $AlTi_4N_3$ and $Al_2Ti_3N_2$ ternary nitrides. Chem. Phys. Lett. **865**, 141930 (2025)
22. Wang, K., Zhang, X., Wang, F.: Impact of TM elements (TM = Cr, Mn, Ti, Sc) doped on the electronic and mechanical properties of ZrAlNi intermetallics. Phys. Lett. A **533**, 130215 (2025)
23. Bouferrache, K., Ghebouli, M.A., Ghebouli, B., Fatmi, M., Ahmed, S.I.: Organic–inorganic hexahalometalate-crystal semiconductor K_2(Sn, Se, Te)Br_6 hybrid double perovskites for solar energy applications. RSC Adv **15**, 11923–11933 (2025)
24. Gueridi, B., Bouferrache, K., Ghebouli, M.A., Rouabah, F., Slimani, Y., Chihi, T., Fatmi, M., Ghebouli, B., Bouandas, H., Habila, M., Benali, A.: Physical properties of rutile-TiO_2 nanoparticles and effect on PVA/SiO_2 hybrid films synthesized by sol-gel method. High Energy Density Phys **52**, 101122 (2024)
25. Fatmi, M., Bouferrache, K., Ghebouli, M.A., Ghebouli, B., Alanazi, F.K., Albaqami, M.D., Mohammad, S., Benali, A.: High performance double perovskites of $Cs_2InAgBr_6$ and $Cs_2InAgCl_6$: structural, electronic, optical and thermoelectric properties for next generation photovoltaics. Sci. Rep. **15**, 20851 (2025)
26. Blanco, M.A., Francisco, E., Luaña, V.: Computational methods in solid state chemistry. Comput. Phys. Commun. **158**, 57 (2004)
27. Limpijumnong, S., Lambrecht, W.R.L.: Electronic structure of spinel compounds. Phys. Rev. B **63**, 104103 (2001)
28. G. Tourné , J. Schaffner, B. Cros, C. R. Seances Acad. Sci., Ser. C **272** (1971) 1219–1221.
29. Sato, T., Morita, N., Shimada, M.: Synthesis and Electrical Properties of LixMg1−xM2O4 (M = Ti, V) (0 ≦ × ≦ 1.0). Phys. Status Solidi A **91**, K81 (1985)
30. Ebbinghaus, S.G., Hanss, J., Klemm, M., Horn, S.: J. Alloys Compd. **370**, 75–79 (2004)
31. Ghebouli, B., Ghebouli, M.A., Chihi, T., Fatmi, M., Boucetta, S., Reffas, M.: First-principles study of structural, elastic, electronic and optical properties of SrMO3 (M=Ti and Sn). Solid State Commun **149**(47–48), 2244–2249 (2009)
32. Born, M., Huang, K.: Dynamical theory of crystal lattices. Oxford University Press, Oxford (1954)
33. Voigt, W.: Lehrbuch der Kristallphysik. Teubner, Leipzig (1928)
34. Reuss, A.: Berechnung der Fließgrenze von Mischkristallen auf Grund der Plastizitätsbedingung für Einkristalle. ZAMM **9**, 49 (1929)
35. Hill, R.: The elastic behaviour of a crystalline aggregate. Proc. Phys. Soc. Sect. A **65**, 349 (1952)
36. Hill, R.: Elastic properties of reinforced solids: some theoretical principles. J. Mech. Phys. Solids **11**, 357 (1963)